

LOW-ENERGY ELECTRON-POSITRON COLLIDER TO SEARCH AND STUDY $(\mu^+\mu^-)$ BOUND STATE

A.V. Bogomyagkov, V.P. Druzhinin, V.A. Kiselev, V.V. Kobets, A.A. Krasnov,
E.B. Levichev, A.I. Milstein, N.Y. Muchnoi, I.N. Okunev, Y.A. Pupkov,
S.S. Serednyakov, S.V. Sinyatkin

BINP, Novosibirsk

Dimuonium

- Dimuonium, bimuonium or true muonium is a lepton atom ($\mu^+\mu^-$).
- From 6 leptonic atoms (e^+e^-), (μ^+e^-), ($\mu^+\mu^-$), (τ^+e^-), ($\tau^+\mu^-$), ($\tau^+\tau^-$) only two (e^+e^-), (μ^+e^-) were observed.
- Dimuonium is pure QED system (no strong interaction, calculable).
- Very compact (large m_μ), more sensitive to new physics than other exotic atoms.

Why dimuonium?

- Observation of the new classical QED object.
- QED test in the new regime.
- Experimental challenge leads to development of new techniques.
- Tests of muon properties are motivated by
 - 3.5σ difference between $(g-2)_\mu$ measurement and SM prediction,
 - discrepancies in the proton charge radius in muonic hydrogen,
 - hints of lepton-universality violation in rare B decays (LHCb), $B^+ \rightarrow K^+ e^+ e^-$ and $B^+ \rightarrow K^+ \mu^+ \mu^-$.

Some references

- V.N.Baier and V.S.Synakh, Bimuonium production in electron-positron collisions, SOVIET PHYSICS JETP, **14**, № 5, 1962, pp.1122-1125
 - *Properties of the bound state, probability of observation*
- S.J. Brodsky and R.F. Lebed. Production of the Smallest QED Atom: True Muonium ($\mu^+\mu^-$). Phys. Rev. Lett., 102:213401, 2009
 - *Very large crossing angle in order to eliminate background*
- H. Lamm and R.F. Lebed, True Muonium ($\mu^+\mu^-$) on the Light Front, arXiv 1311.3245v3, 12 Nov 2014
 - *Spectrum*
- H. Lamm, True muonium: the atom that has it all, arXiv 1509.09306v1, 30 Sep 2016
 - *Novel properties*

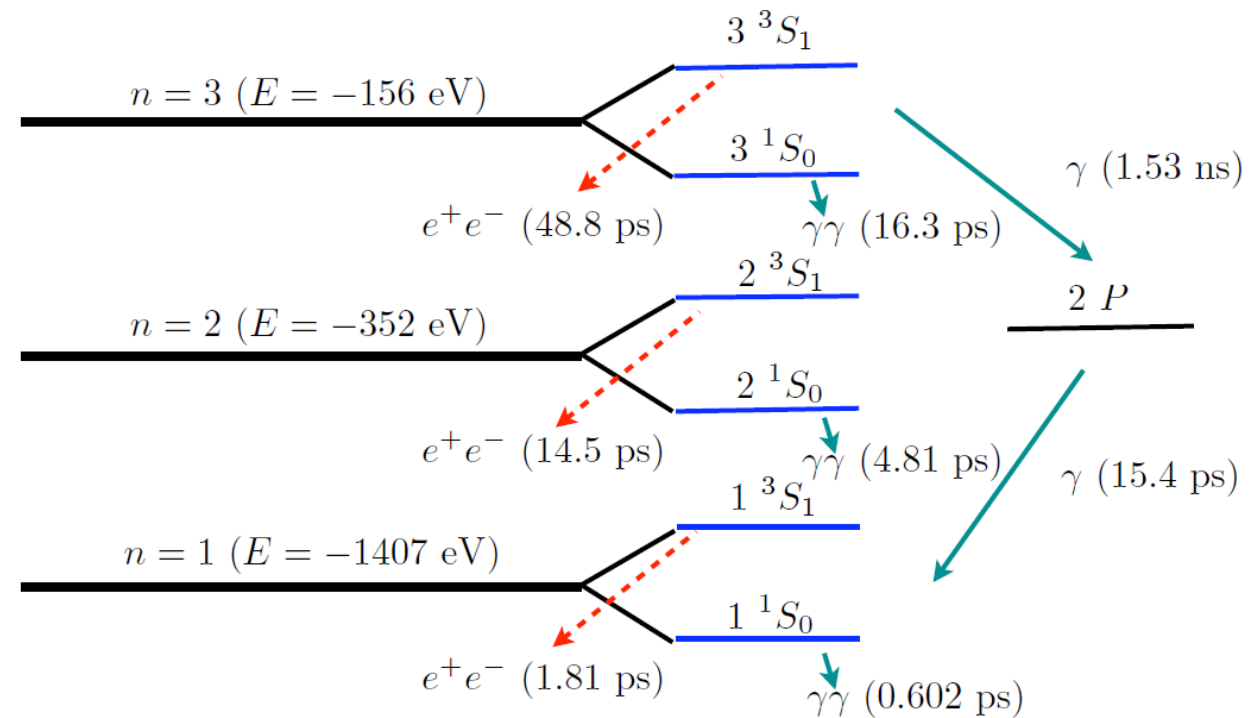
Dimuonium properties

- Mass
 $M_{\mu\mu} = 2 \times 105.7 \text{ MeV} - 1.4 \text{ keV}$
- Bohr radius
 $R_{\mu\mu} = 512 \text{ fm}$
 $R_{ee} = 106000 \text{ fm}$
- Muon lifetime $2.2 \mu\text{s}$
- 3S_1 states have photon quantum numbers ($J^{PC} = 1^{--}$); therefore could be produced in e^+e^- collisions

Dimuonium energy levels diagram

S.J. Brodsky, R.F. Lebed, Phys. Rev. Lett., 102:213401, 2009

$n = \infty (E = 0)$



Dimuonium production cross section

- Production of $n \ ^3S_1$ in the $e^+e^- \rightarrow (\mu^+\mu^-) \rightarrow e^+e^-$

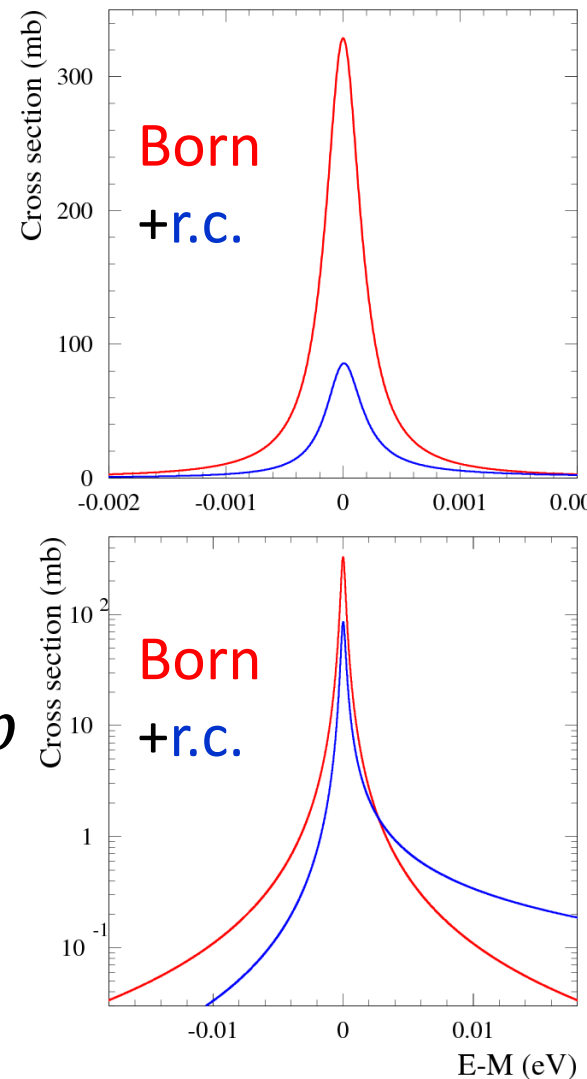
- 1 3S_1 : $\sigma(m_{\mu\mu}) \approx \frac{12\pi}{m_{\mu\mu}^2} \sqrt{\frac{\pi}{8}} \frac{\Gamma_{ee}}{\sigma_M} \approx 0.2 \frac{\Gamma_{ee}}{\sigma_M}$

where σ_M is center-of-mass energy spread

- For different collision schemes

$$\frac{\Gamma_{ee}}{\sigma_M} = \frac{0.37 \times 10^{-6} \text{ keV}}{(7 \div 400) \text{ keV}} \approx (1 \div 50) \times 10^{-9}, \sigma(m_{\mu\mu}) = 0.15 \div 7 \text{ nb}$$

- Background: elastic $e^+e^- \rightarrow e^+e^-$ scattering
 - For crossing angle $45^\circ \div 135^\circ \sigma_{Bhabha} = 22000 \text{ nb}$
- Background/signal* = $(5 \div 210) \times 10^3$
- Background suppression is possible if decay point is separated from the origin point (decay path 1 3S_1 : $c\tau = 540 \mu\text{m}$)



Head-on e+e- collision

$E_{beam} = 100 \div 150 \text{ MeV}$

Collision monochromatization a la Reniery:

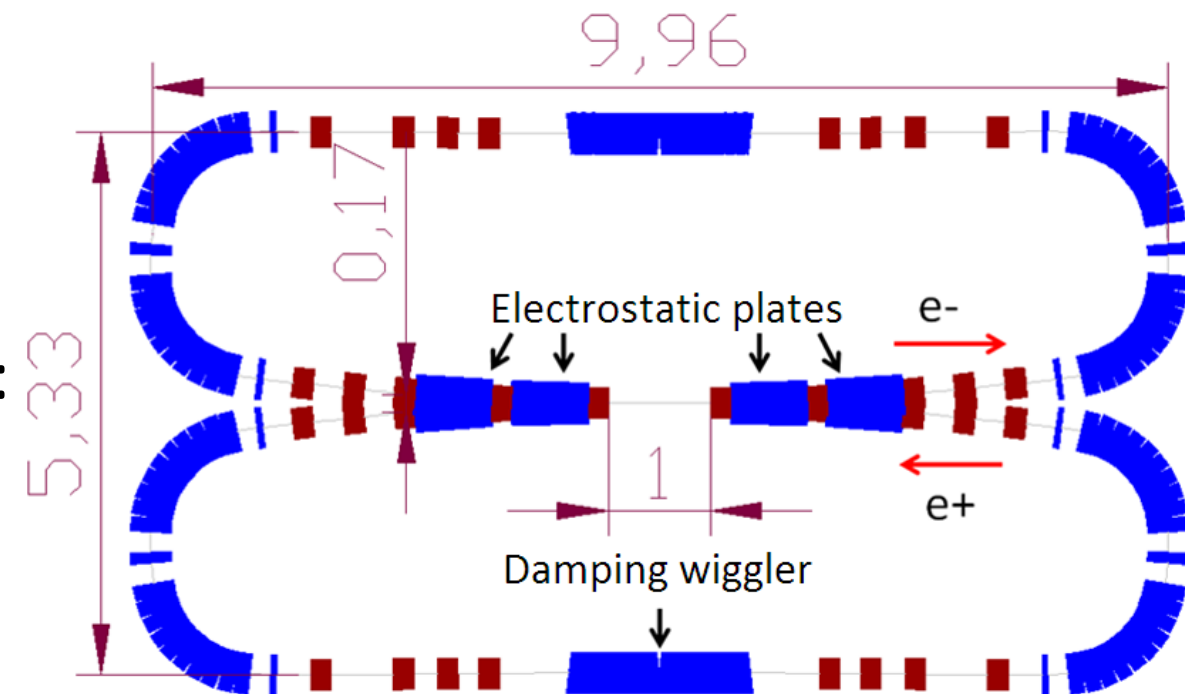
10 keV invariant mass resolution

$L \approx 10^{30} \text{ cm}^{-2}\text{s}^{-1}$ ($\sim 50 (\mu^+\mu^-)$ /hour).

Observation of the dimuonium
by searching for X-rays from $(\mu^+\mu^-)$
Bohr transitions such as $2P \rightarrow 1S$ (J.W.Moffat).

Failed due to large background.

Large crossing angle proposed by S.J.Brodsky and R.F.Lebed.

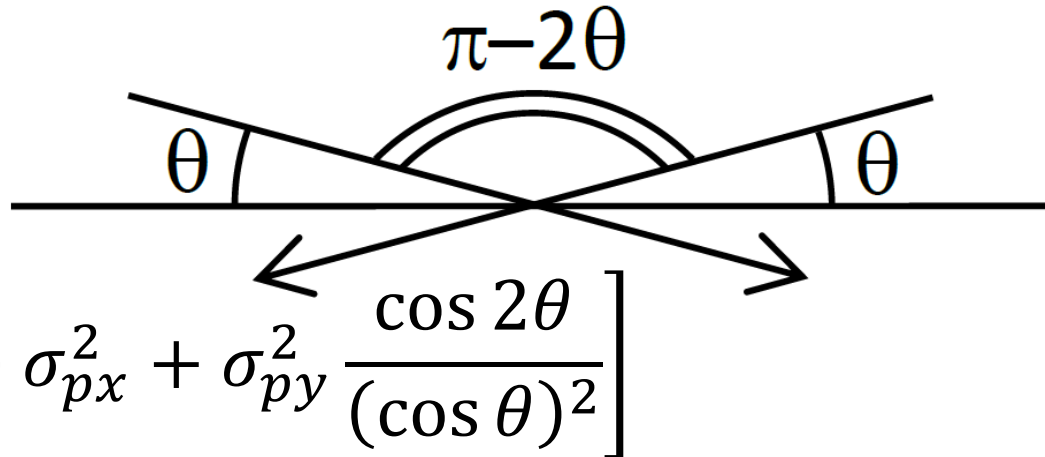


<https://eventbooking.stfc.ac.uk/uploads/eefact/mumutron-eefact2016-2.pptx>

Large angle beam crossing

Invariant mass

$$\langle M \rangle = 2E_0 \cos \theta - \frac{E_0}{2} \cos \theta \left[\sigma_\delta^2 + \sigma_{px}^2 + \sigma_{py}^2 \frac{\cos 2\theta}{(\cos \theta)^2} \right]$$



Invariant mass resolution

$$\sigma_M^2 = 2E_0^2 [\sigma_\delta^2 (\cos \theta)^2 + \sigma_{px}^2 (\sin \theta)^2]$$

Luminosity ($\varphi = \sigma_z \tan \theta / \sigma_x$)

$$\mathcal{L}_0 = \frac{N_1 N_2}{4\pi \sigma_y \sigma_x \sqrt{1 + \varphi^2}} f_0 N_b \approx \frac{N_1 N_2}{4\pi \sigma_y \sigma_z \tan \theta} f_0 N_b$$

Peak production rate

$$\dot{N}_{\mu\mu} \approx \frac{\Gamma_{\mu\mu} \sigma_{\mu\mu} \mathcal{L}_0}{2\sqrt{\pi} \sigma_M}$$

Background

Decay length ($\mu^+ \mu^- (1\ ^3S_1) \rightarrow e^+ e^-)$

$$OA = l = c \tau_{0,\mu\mu} \beta_{\mu\mu} \gamma_{\mu\mu} = c \tau_{0,\mu\mu} \tan \theta$$

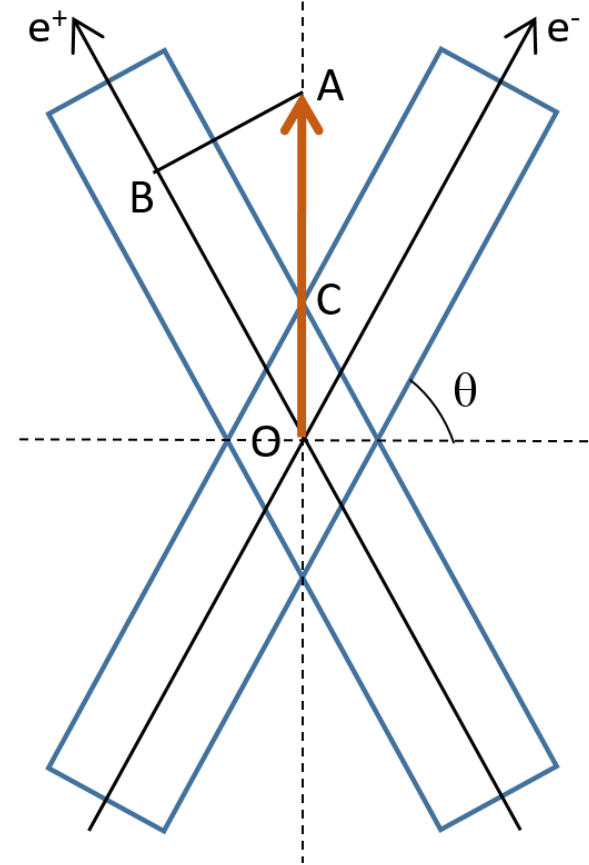
Background: density of beam particles

$$N_1 \propto \exp(-n_x^2/2)$$

$$n_x = \frac{AB}{\sigma_x} = \frac{l \cos \theta}{\sigma_x} = \frac{c \tau_{0,\mu\mu}}{\sigma_x} \sin \theta$$

Signal to background ratio

$$\frac{\dot{N}_{\mu\mu}}{\dot{N}_{ee}} \propto \frac{\exp \left[\frac{c^2 \tau_{0,\mu\mu}^2}{\sigma_x^2} \sin^2 \theta \right]}{\sqrt{\sigma_\delta^2 \cos^2 \theta + (\sigma_x^2 / \beta_x^2) \sin^2 \theta}}$$



Beam-beam effects with large crossing angle

Beam-beam tuneshift

$$\xi_z = -\frac{N r_e}{2\pi\gamma} \frac{\alpha}{|\alpha| \sigma_\delta \sigma_z} \frac{\varphi^2}{1 + \varphi^2}$$

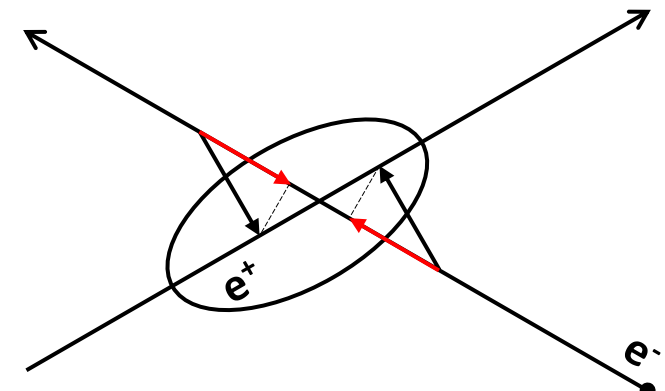
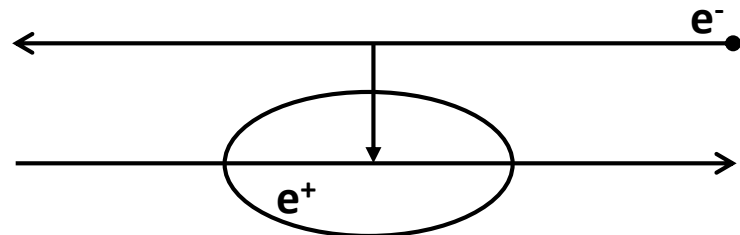
Hamiltonian

$$\mathcal{H} = -\alpha \frac{p_z^2}{2} - \frac{\nu_s^2}{\alpha R^2} \frac{z^2}{2} - \frac{2\xi_z \nu_s}{\alpha R^2} \frac{z^2}{2}$$

Population limit for $\alpha > 0$

$$N < \frac{2\pi R \gamma \alpha \sigma_\delta^2}{r_e} \frac{2}{2}$$

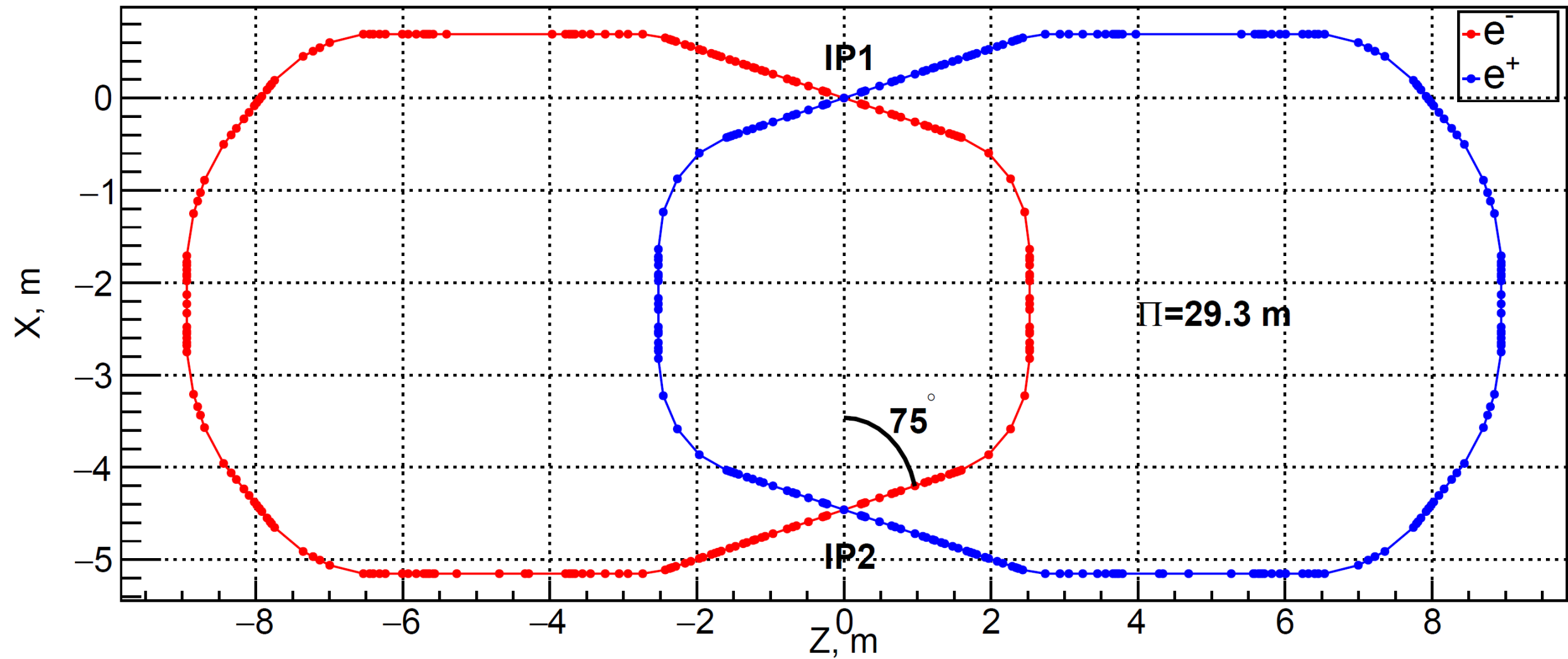
$\alpha < 0$ has been studied at KEKB and at DAΦNE, no large currents, no luminosity due to microwave instability



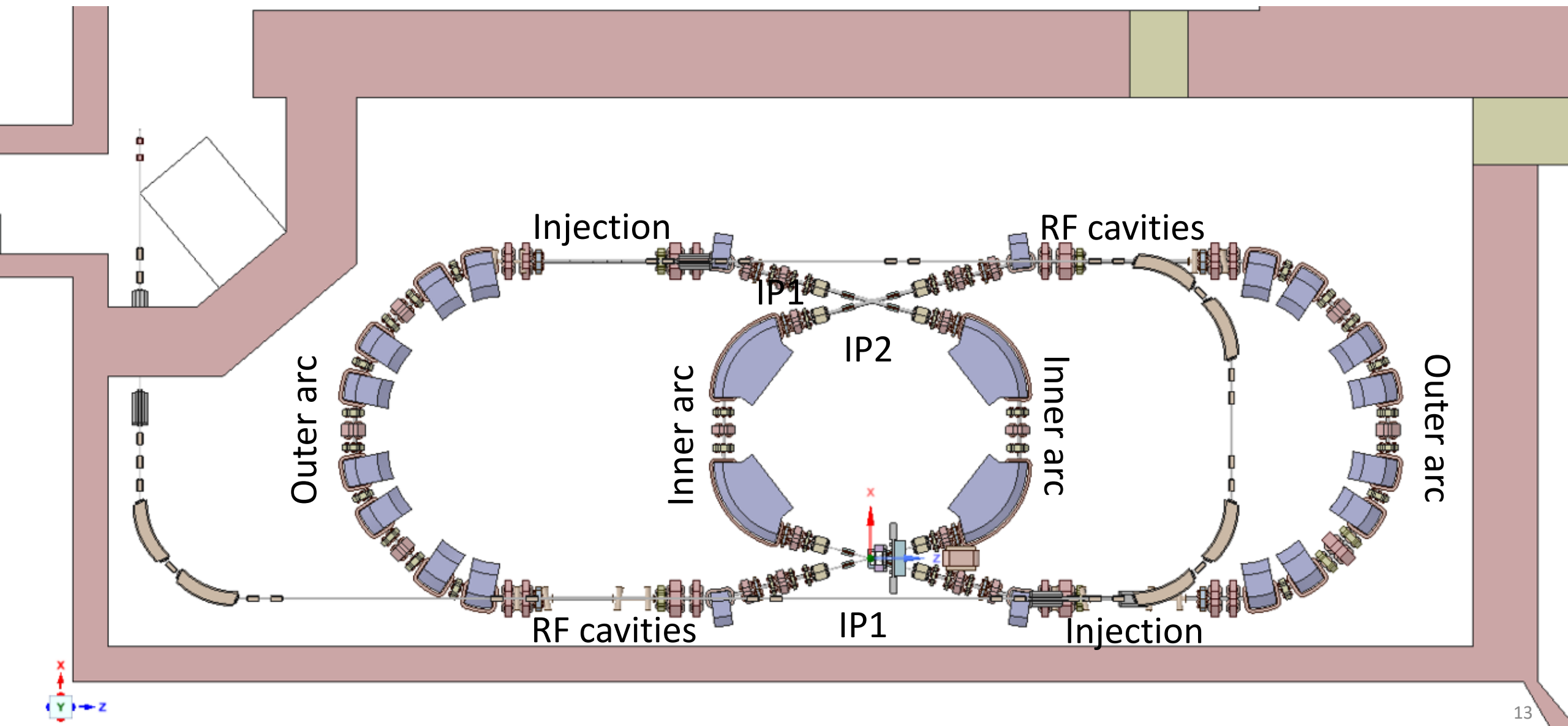
Accelerator requirements

- Large positive momentum compaction (small circumference)
- Large crossing angle with small vertical beta function gives high luminosity (similar to crab waist)
- Large crossing angle 75° provides comfortable beam energy (e^+ production) and decay length
 - beam energy $E_b = 408 \text{ MeV}$
 - decay length $l(\mu^+ \mu^- (1 \ ^3S_1)) = 2 \text{ mm}$
- Higher signal to noise ratio requires $\sigma_x < c \tau_{0,\mu\mu} = 0.54 \text{ mm}$
- Horizontal beam divergence contributes significant part in invariant mass resolution; therefore, low horizontal emittance
- Reverse of the beam direction provides 15° crossing angle and allows to study c.m. energy range from η to η' mesons (550-960 MeV)

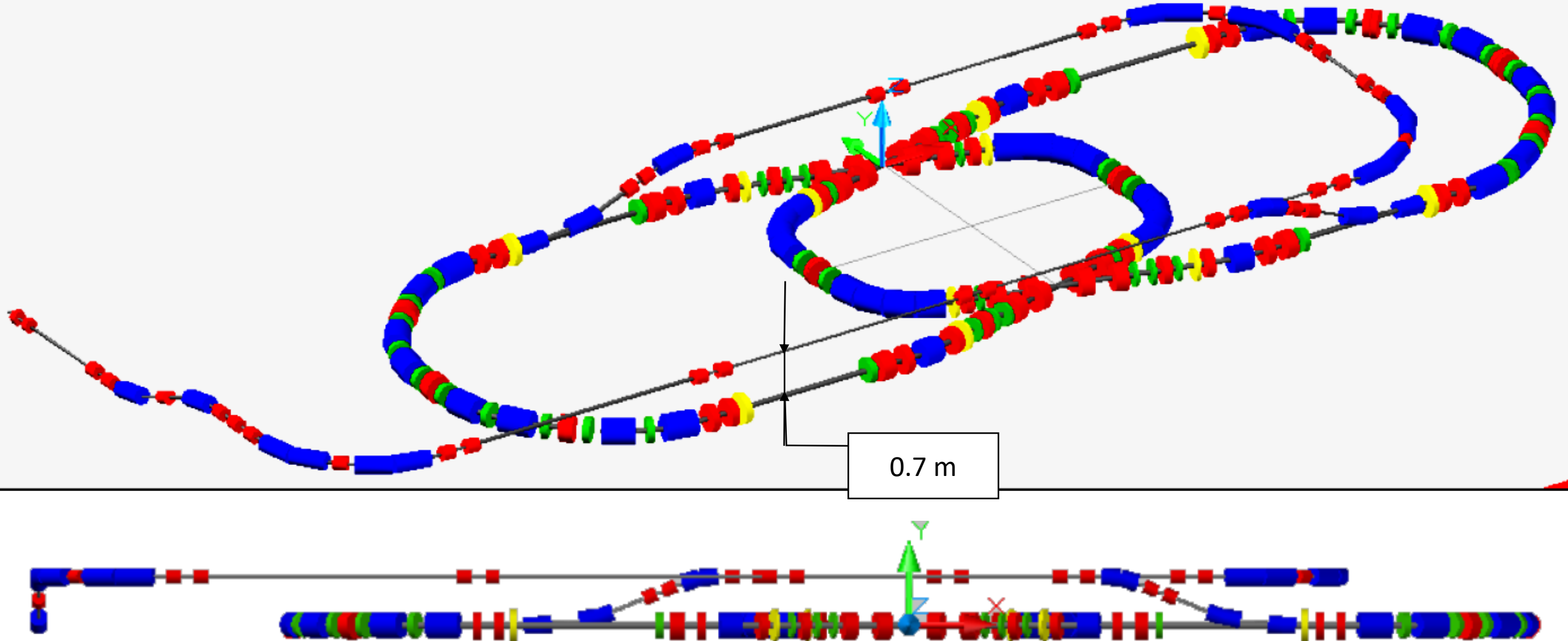
Collider: overview



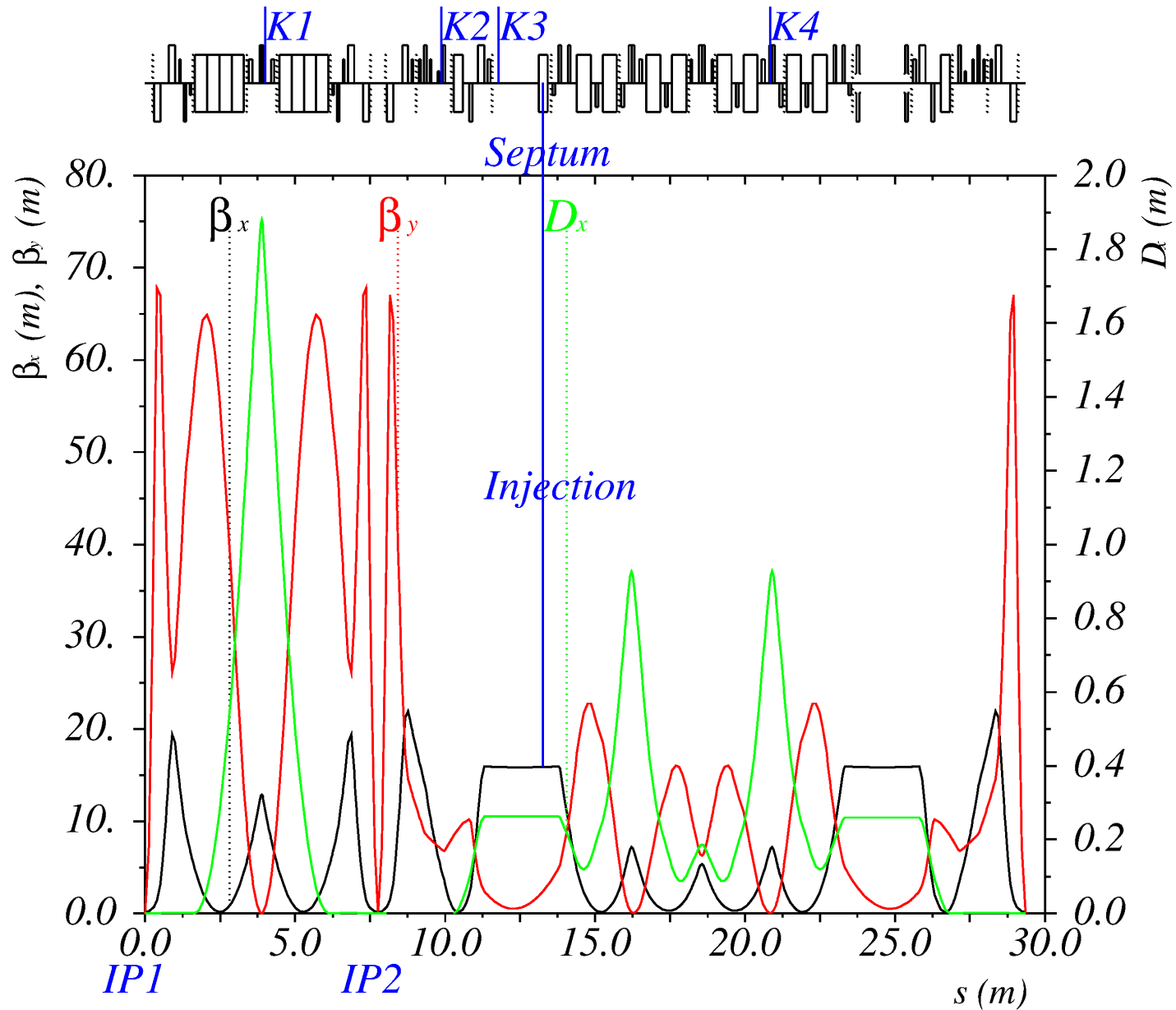
Collider: overview



Injection channels

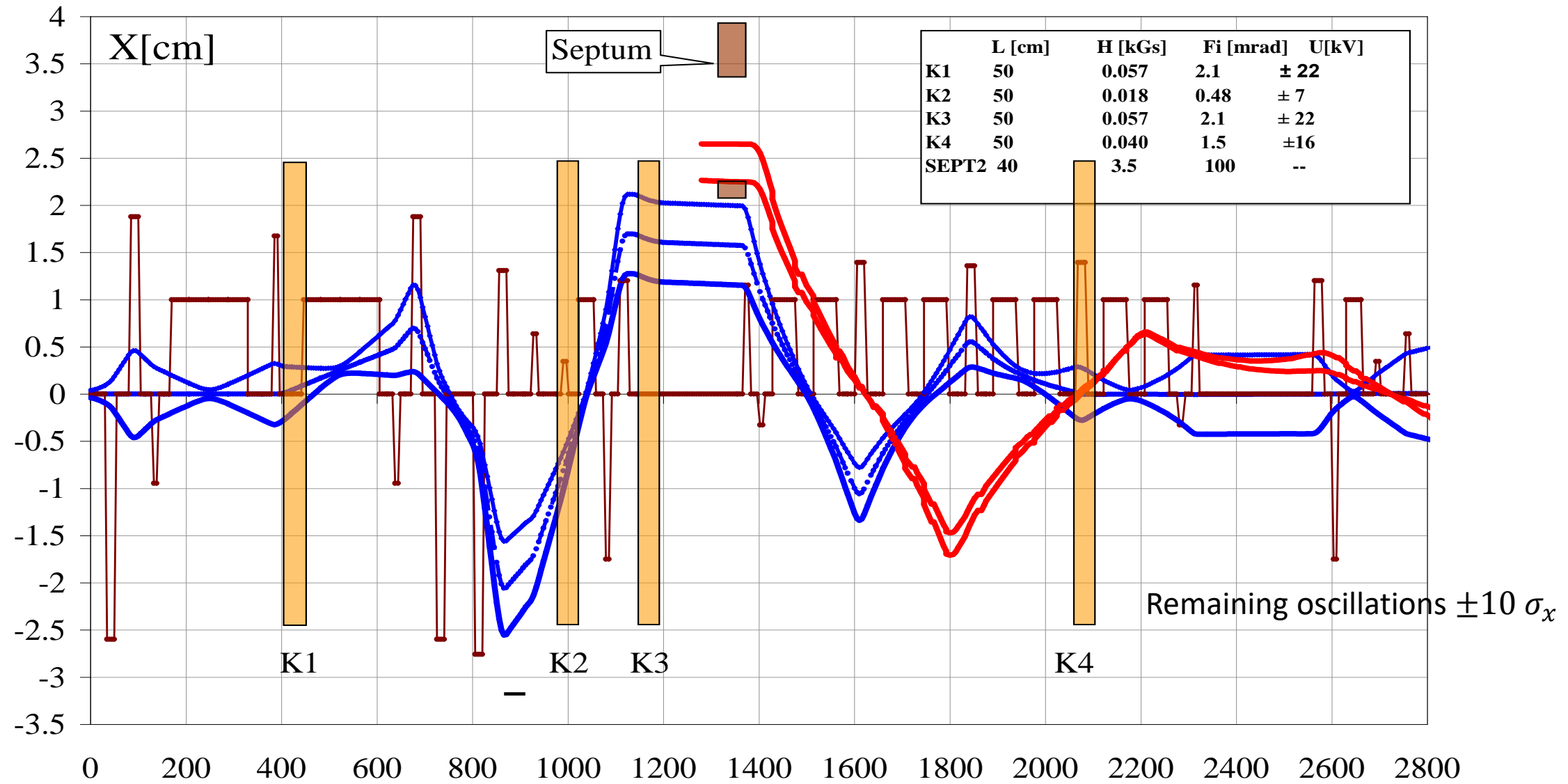


Injection optics

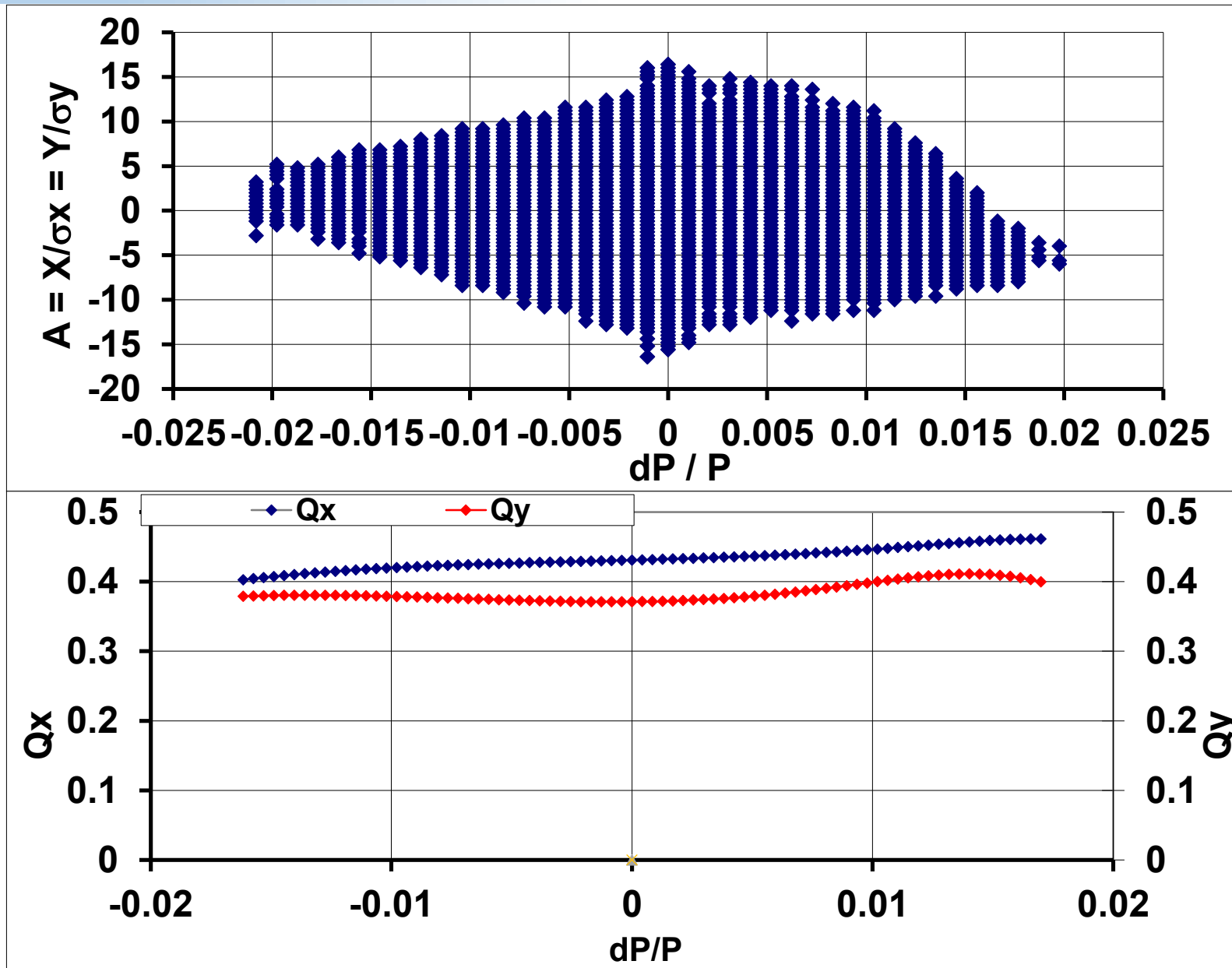


- One turn injection in the horizontal plane
- K1 – K4 – running wave kickers
- Septum – Lambertson injection magnet

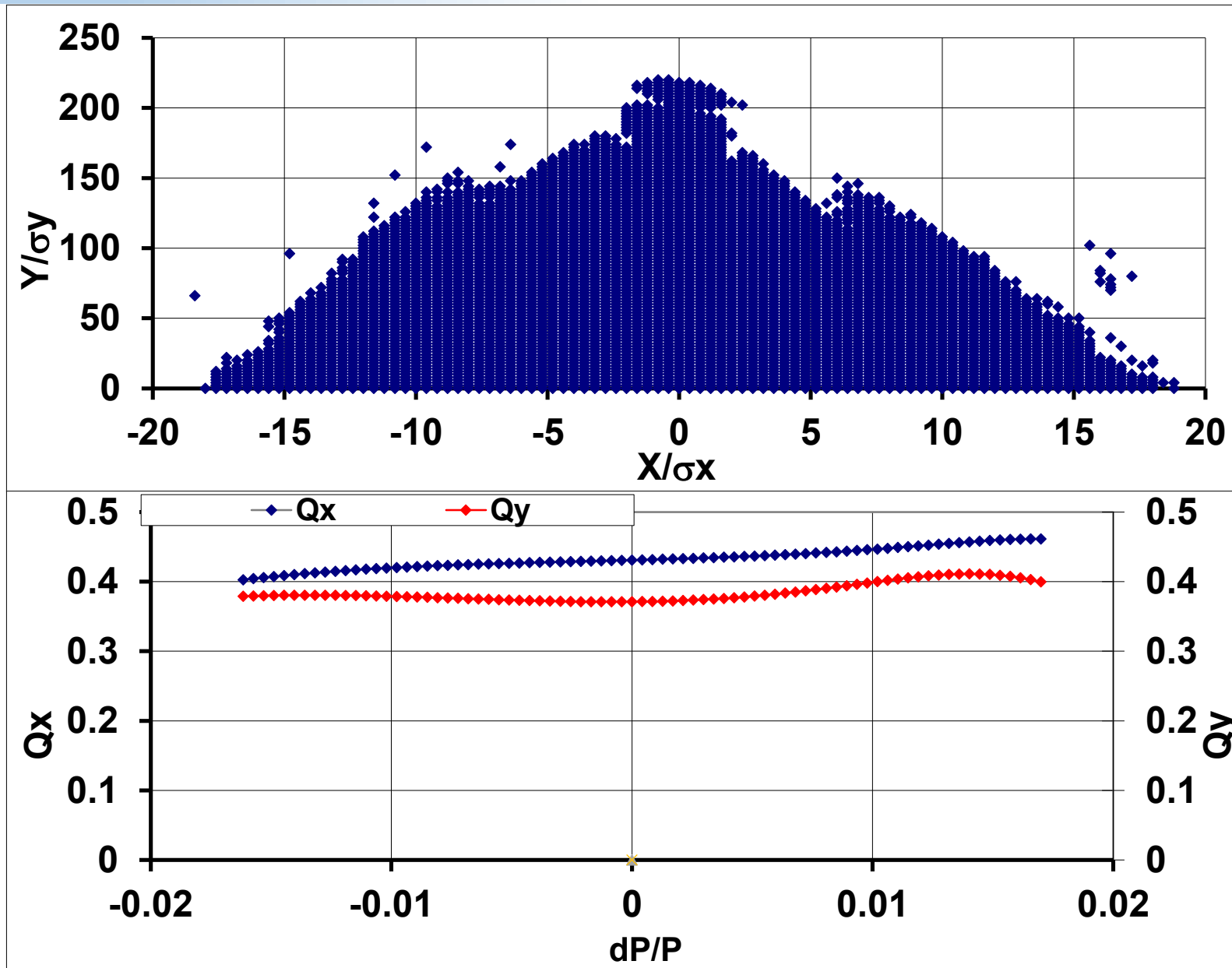
Injection trajectories



Dynamic aperture and energy acceptance

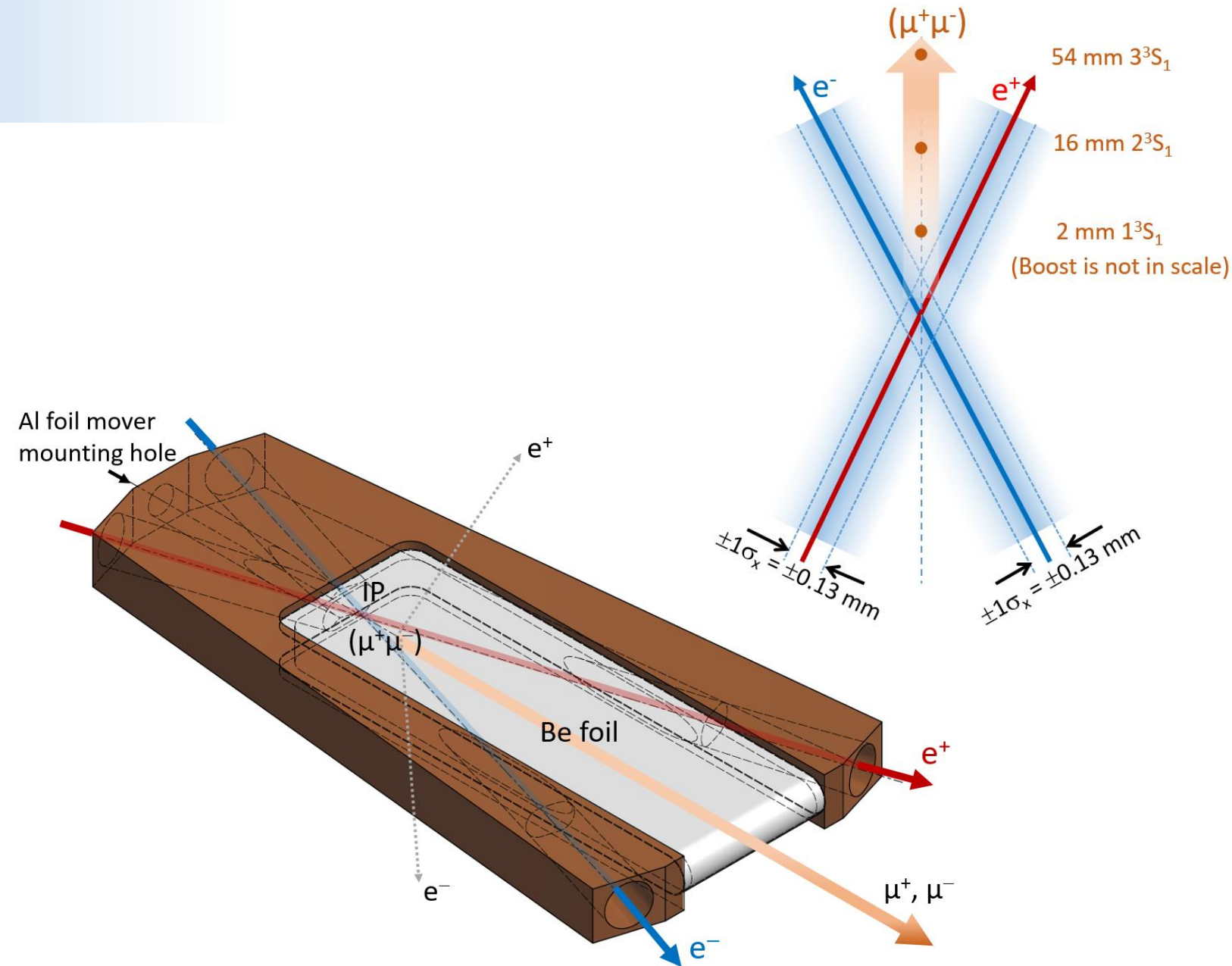


Dynamic aperture and energy acceptance



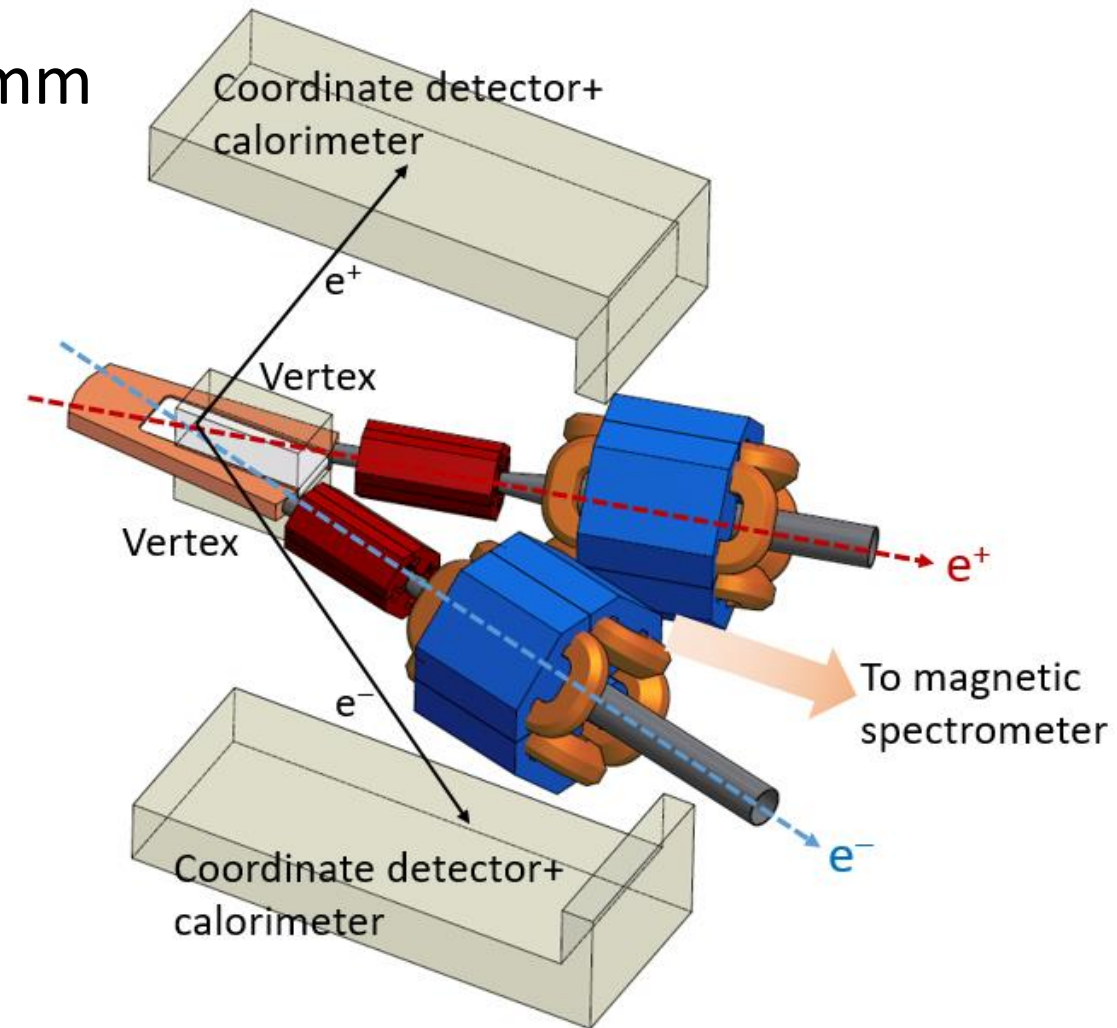
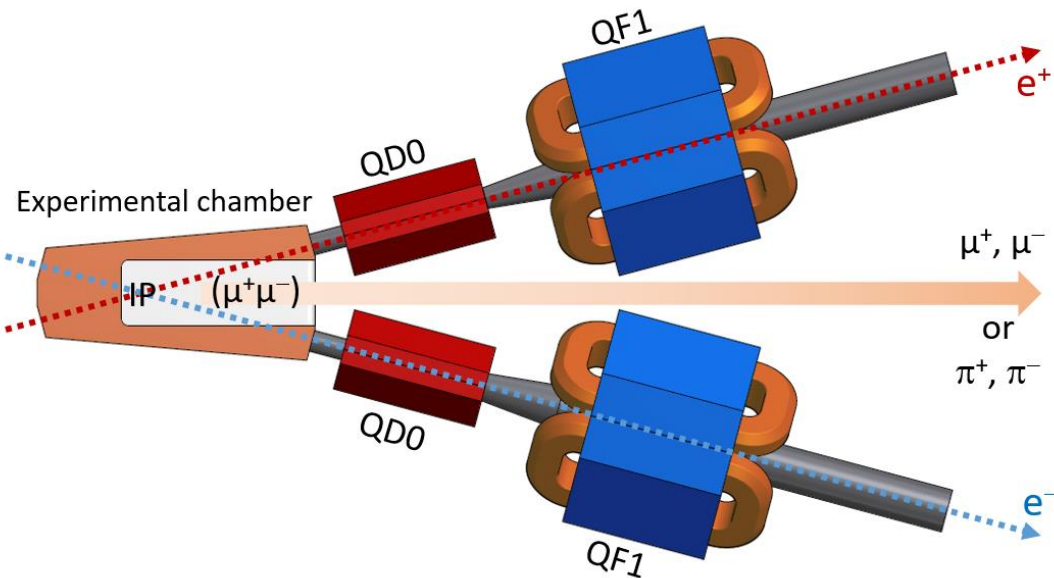
Interaction region

- Experimental chamber:
flat box with 0.5-mm-thick beryllium windows
on the top and on the
bottom allowing passage
of e^\pm produced by the
dimuonium atoms decay.
- Detector: tracking
systems around the
median plane, magnetic
spectrometer



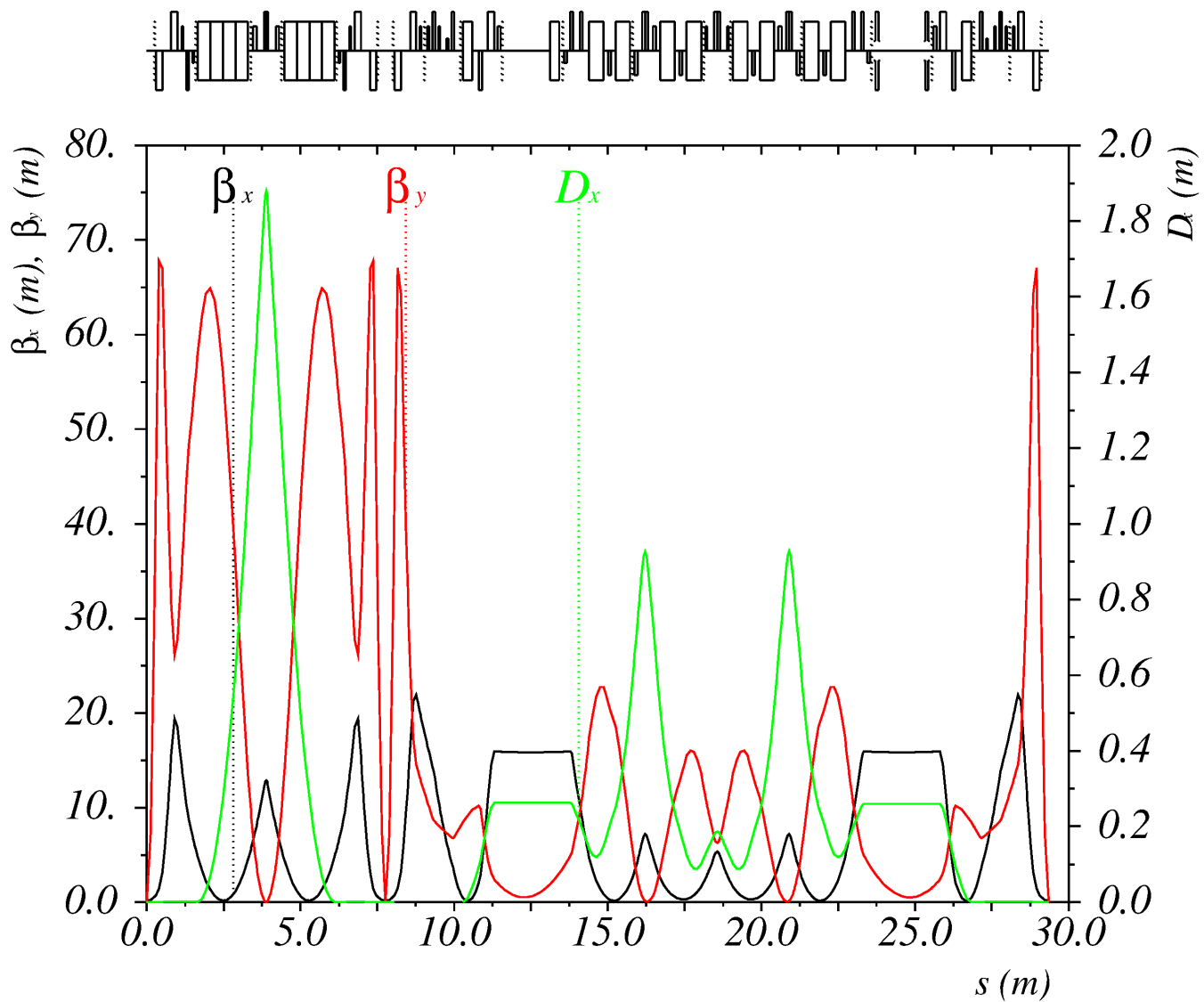
Interaction region

- QD0: permanent magnet, $G=-35$ T/m, \varnothing 30mm
- QD/QF1: electromagnet



Collider: optics

Beam energy	408 MeV
Circumference	29.35 m
Momentum compaction	5.8×10^{-2}
Bunch intensity	$3.5 \times 10^{10} / 57 \text{ mA}$
Horizontal emittance	30 nm 65 nm (IBS)
Energy spread	3.7×10^{-4} 8.7×10^{-4} (IBS)
β_x / β_y	150 mm / 2 mm
Luminosity	$2.8 \times 10^{30} \text{ cm}^{-2}\text{s}^{-1}$, Nb=1 $8.3 \times 10^{31} \text{ cm}^{-2}\text{s}^{-1}$, Nb=30



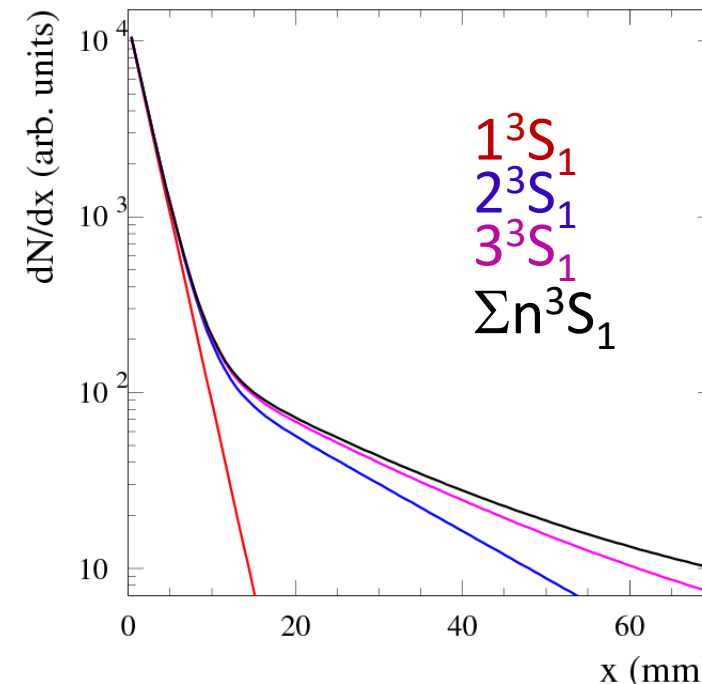
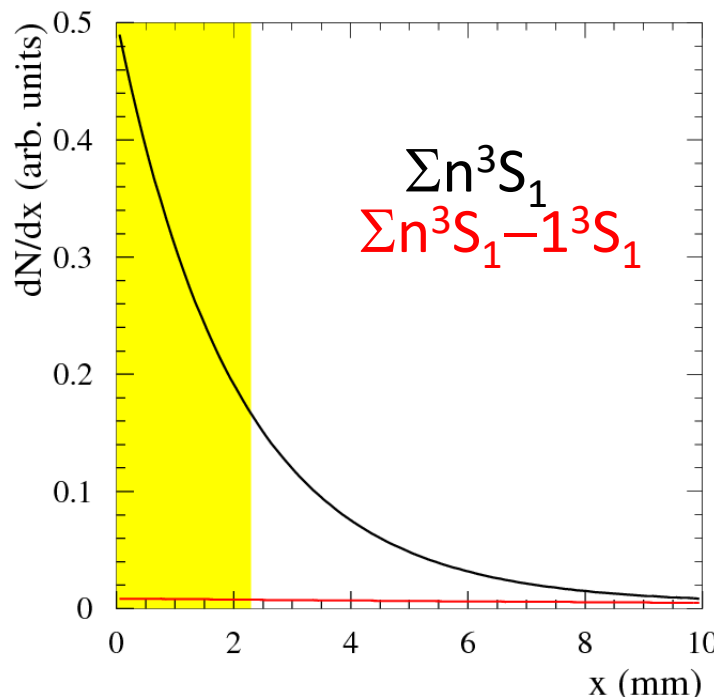
Collider: parameters

RF frequency	347.29 MHz	Beam energy	408.225 MeV
RF harmonic	34	Invariant mass (M)	211.315 MeV
RF voltage	510 kV	σ_M	383 keV
RF acceptance	2%	σ_M/M	1.8×10^{-3}
Synchrotron tune	1.96×10^{-2}	IP beam divergence	6.4×10^{-4} (hor)
Damping partition	1.6 (hor) 1.4 (lon)	Energy spread	3.7×10^{-4} 8.7×10^{-4} (IBS)
Damping times	25 ms (hor) 40 ms (ver) 28 ms (lon)	Beam-beam tune shift	2×10^{-6} (hor) 1.1×10^{-3} (ver) -2×10^{-3} (lon)
Bunch length	5.1 mm 12 mm (IBS)	IP beam size at IP	$97 \mu\text{m} (\sigma_x \text{ IBS})$ $264 \mu\text{m} (\sigma_x / \sqrt{2} \cos \theta)$

Dimuonium production and distribution

- Detection efficiency is about 15% (2 IPs)
- $\beta\gamma c\tau = 2.03 \text{ mm}$
- $\sigma_x(\text{IP}) = \sigma_x / (\sqrt{2} \cos \theta) = 280 \mu\text{m}$
- Detector vertex resolution is $150 \mu\text{m}$
- Total $\sigma_{vtx} = 320 \mu\text{m}$
- 6.25σ background suppression with vertex position $x > 2 \text{ mm}$

$\mu^+ \mu^-$ rate	1 hour	4 months
$x > 2 \text{ mm}$	1S/2S/3S	4.7/1.4/0.5



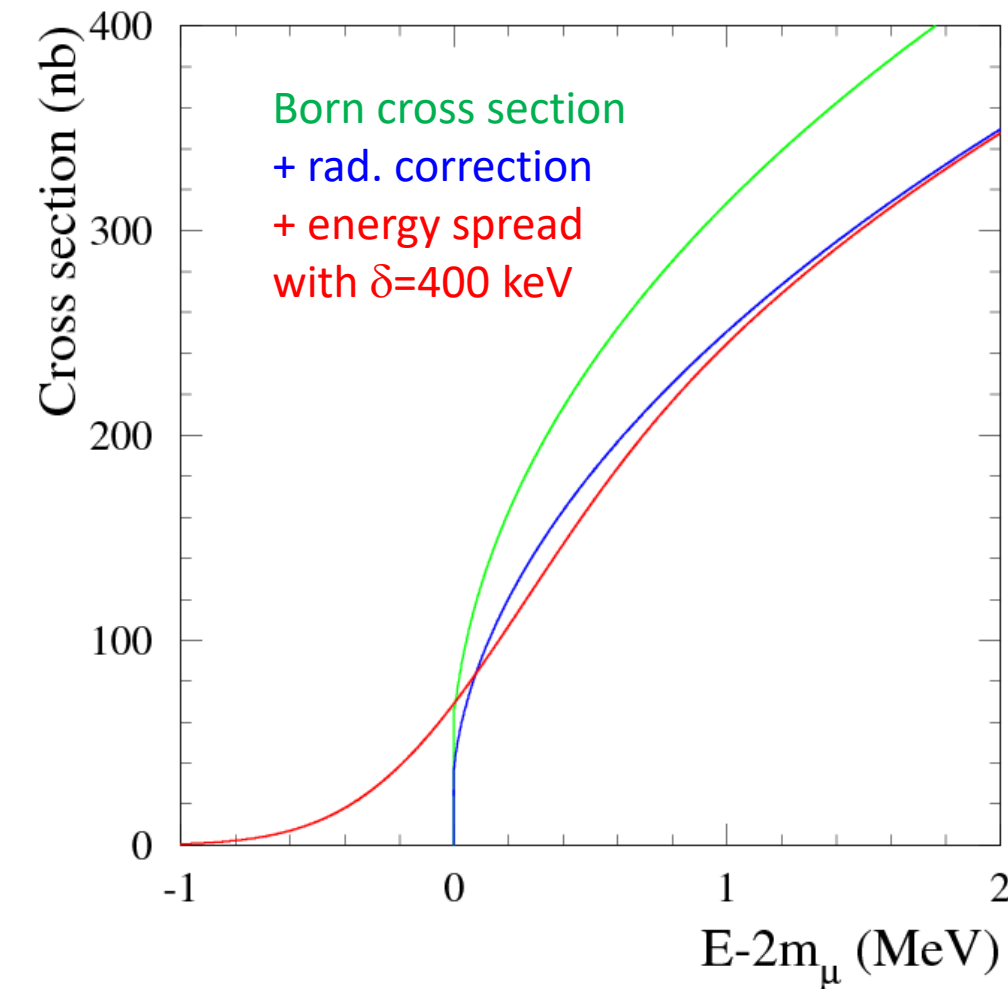
Experiments: what can we measure?

- From the fit of the decay vertex distribution
 - *dimuonium production rate (Γ_{ee}) of 1S (2% for 10^7 s), 2S(15%), 3S(30%)*
 - *dimuonium decay lengths with the same accuracy*
- Dimuonium interaction with a thin foil (30 μm Al) allows
 - *measurement of the breakup probability*
 - *measurement 1S-2P transition probabilities*
 - *2P lifetime*
- Laser spectroscopy (?)
 - ΔE (2S-2P) (laser $\lambda \approx 100\mu\text{m}$)
 - *2P lifetime*

Experiments: $e^+e^- \rightarrow \mu^+\mu^-$ near threshold

Coulomb interaction in the final state leads to nonzero cross section at the threshold; therefore,

- Background-free measurement of the cross section near the threshold, requires magnetic spectrometer
- Precision measurement of the SSSG-factor
- C.M. energy and its spread calibration
- The same technique may be used for $e^+e^- \rightarrow \pi^+\pi^-$



Experiments: 15° crossing angle

- This region (c.m. 550-960 MeV) of ρ and ω resonances is important for SM $(g-2)_\mu$ calculation
- $e^+e^- \rightarrow \pi^+\pi^-$ cross section measurement with unlimited statistics
- Precision measurements of other hadronic cross sections ($e^+e^- \rightarrow \pi^+\pi^-\pi^0, \pi^0\gamma, \eta\gamma, \pi^0\pi^0\gamma, 4\pi, \dots$)
- Rare processes $e^+e^- \rightarrow \eta, \eta'$
- Two-photon processes $\gamma\gamma \rightarrow \pi^0, \pi\pi, \eta$
- Measurement of meson-photon transition form factors

Reverse beam: 15° crossing angle

Beam energy	283.59 MeV (η)	495.78 MeV (η')
Invariant mass (M)	547.86 MeV	957.76 MeV
$\sigma_M (\sigma_M/M)$	420 keV (7.7×10^{-4})	580 keV (6.1×10^{-4})
Energy spread	2.8×10^{-4} / 10.6×10^{-4} (IBS)	4.8×10^{-4} / 8.4×10^{-4} (IBS)
IP beam divergence (hor)	8.3×10^{-4}	7.1×10^{-4}
Horizontal emittance	11.4 nm / 105 nm (IBS)	34.8 nm / 75 nm (IBS)
Bunch length	3.7 mm / 14.2 mm (IBS)	6.3 mm / 11 mm (IBS)
Beam-beam ξ (h/v/l)	3×10^{-4} / 1.4×10^{-2} / -2×10^{-3}	3×10^{-4} / 1.3×10^{-2} / -2×10^{-3}
Synchrotron tune	1.67×10^{-2}	1.71×10^{-2}
Luminosity (Nb=1 / 30)	3.3×10^{31} / 9.9×10^{32}	5.2×10^{31} / 1.5×10^{33}

Conclusion

- Collider to observe and study bound state of ($\mu^+\mu^-$)
 - *two rings, large crossing angle*
 - *circumference 29 m, not expensive to build and operate*
 - *luminosity $8 \times 10^{31} \text{ cm}^{-2}\text{s}^{-1}$*
- Reverse of the beam allows experiments in 500-1000 MeV central mass energy range
- Geometry is optimized to fit the present hall.
- Dynamic aperture and energy acceptance are sufficient for injection and beam life time.
- Details are in <https://doi.org/10.1051/epjconf/201818101032>
<https://pos.sissa.it/314/810/pdf> and <https://arxiv.org/abs/1708.05819>
- We started manufacturing of the collider components.

We are open for collaboration and experiments proposals